



HAL
open science

On-site Raman study of artwork: Procedure and illustrative examples

Philippe Colomban

► **To cite this version:**

Philippe Colomban. On-site Raman study of artwork: Procedure and illustrative examples. *Journal of Raman Spectroscopy*, 2018, 49 (6), pp.921-934. 10.1002/jrs.5311 . hal-03940352

HAL Id: hal-03940352

<https://hal.science/hal-03940352>

Submitted on 16 Jan 2023

HAL is a multi-disciplinary open access archive for the deposit and dissemination of scientific research documents, whether they are published or not. The documents may come from teaching and research institutions in France or abroad, or from public or private research centers.

L'archive ouverte pluridisciplinaire **HAL**, est destinée au dépôt et à la diffusion de documents scientifiques de niveau recherche, publiés ou non, émanant des établissements d'enseignement et de recherche français ou étrangers, des laboratoires publics ou privés.

On-site Raman study of artwork: Procedure and illustrative examples

Philippe Colomban

Sorbonne Universités, UPMC Univ Paris 06, UMR 8233, CNRS, MONARIS, F-75005, Paris, France.

Philippe.colomban@upmc.fr

Abstract

Raman microspectroscopy conducted with transportable/mobile instruments allows for the non-invasive identification of amorphous and crystalline phases of ancient masterpieces and outstanding artworks (objects, paintings and décor, building parts, etc.). Resonance Raman spectroscopy detects chromophore and dye traces. On the basis of examples (enamelled glass and pottery, enamelled metal, patinated/corroded metal, stained glass, sculptures, paintings, pastels and drawings) this mini-review discusses the main parameters (laser and optics choice, experimental procedure, etc.) and shows how phase identification contributes to a better understanding of innovant technology exchanges.

Keywords

Cultural Heritage, mobile, glass, pigments, paintings

1. Introduction

Since the beginning of civilisation, emperors, kings and princes have been on the receiving end of exceptionally crafted objects. The first ones were carved from rare minerals: quartz and homologue silicates (rock crystal, carnelian, amethyst, agate, onyx ...), jade, malachite, lapis lazuli, turquoise, ruby, sapphire, etc. These minerals offered a variety of colours, glosses and shapes, of which some were very rare among natural minerals or only found in very minute quantities. Synthetic glass compete with rare coloured minerals and have the advantage of making possible the association of various colours. Egyptian glassmakers and potters already prepared turquoise, red and blue glass/enamels a few millennia ago BCE¹ while Celtic craftsmen prepared vivid blue and red enamels a few centuries ago BCE². Tang potters (7th-10th centuries) first prepared white artefacts exhibiting a gloss similar to those of some marine shells,. Before the development during Ming Dynasty of trading through the maritime Silk Road in replacement of the terrestrial Silk Road,³ these artefacts were very rare, which makes the number of preserved items in public and private collections very limited. The numbers of imported Chinese porcelains increased drastically with the establishment of the Portuguese (16th century) and then Dutch/British Indian (17th century) Companies.⁴ And even more so when European ceramic and glass Factories⁵ were founded after 1750 mainly to satisfy the demand generated by the Elite. Furthermore, the fragility and scarcity of enamelled glass masterpieces has limited the number of surviving objects made before the 16th-18th centuries. Consequently, analytical information on the materials and technologies used to make these precious artefacts is also rare, if not inexistent. For instance, in 1815, H. Davy, – founder of Archaeometric studies with R.A. Ferchault de Réaumur^{6,7} – needed large fragments of murals found in Pompeii and pigments of Egyptian blue for their analysis. More than one hundred years later, in 1922, H.A. Eccles and B. Rackham asked again for several parts of a porcelain service to study the composition of their enamels⁷ (analysis who employed solubilisation, specific element precipitation, drying and weighting of the final product). However, present-day ethics require non-destructive, non-invasive techniques. Moreover, the need to keep precious items in secure areas led to the use of mobile and contactless instruments, while the on-going miniaturisation of laser, spectrometer, detectors and computer⁸ led to the popularisation of Raman mobile set-ups to study Cultural Heritages.^{7,9-12} The collection of Raman data for paintings is more complex: paintings are unique and fragile which limits their handling, and the pictorial layers are generally covered with one or more layers of varnish, a material that gives rise to strong fluorescence phenomenon covering Raman signal.¹³ Consequently, section analyses of (micronic) scales obtained by sampling or collected after simply falling during handling or

restoration is needed. Obviously, immovable artefacts (Rock art, frescoes, stained glass, building, sculptures, statues, etc.) also require the use of transportable instruments.

Reviews dealing with Cultural studies using Raman microspectroscopy and/or other mobile analytic techniques (XRF, IR, LIBS, FORS) have already been the subject of publications.⁹⁻¹² And the advantages of Raman microspectroscopy in the field of Cultural Heritage studies have been widely discussed. Namely, i) no contact and preparation of the artefact are needed, ii) the probe being the chemical bond, the technique is efficient to study both crystalline and amorphous phases, iii) the best spatial resolution is sub-micronic, and iv) the process is highly efficient in detecting dye and pigments. Pigments were among the first materials to be studied when the first Raman Molecular Examiner (Mole) appeared in 1970's,¹⁴⁻¹⁶ especially those used in illuminated manuscripts¹⁶⁻¹⁹ or in wall paintings (frescoes).²⁰⁻²⁸ However, those pigments generally consisted in powdered minerals with high purity, almost free of organic binders generating strong fluorescence. The sampling (a few μm^2 to a few cm^2) and study was performed at a laboratory that allowed for the building of databases.^{9,18,29.}

We present here a mini-review of Raman studies of Cultural Heritage masterpieces performed on-site with mobile set-ups. Measurements with mobile Raman set-up started around 2004³⁰⁻³³ when air-cooled lasers became available for LIDAR studies.^{34,35} Some papers have already discussed the use of transportable, mobile/portable and handheld/palm instruments³⁶⁻⁴². Special attention will be given to the experimental procedures (collection of the spectra procedure, choice of the laser wavelength and of the optics) and to the importance of some spectrometer characteristics (spectral and spatial/volume resolution, detection of broad bands, band area measurements, etc.) in order to be able to study the vibrational signature of complex multiphased materials made of both broad and narrow components. Then, we will use representative examples to show the potential and the drawbacks encountered in the study of almost 'organic-free' (glass, glaze, pottery, corroded/patinated metal) and of organic-containing artefacts (paintings, lacquer). We will underline that Raman (micro) spectroscopy cannot be considered an analytical technique since the understanding of the interaction of lights with solids, especially coloured materials, requires a good knowledge of solid state physics and chemistry. Many of the information presented is available in textbooks describing light-matter interactions but have not been considered in light of the constraints imposed by a mobile Raman set-up.

2. Experimental and Procedures

Choice of the laser wavelength

The Raman scattering intensity depends on laser wavelength (with exponent 4), laser intensity and detector (and optics) efficiency. Blue laser is the most appropriate wavelength to get a strong spectrum under low illuminating power (optics, laser sources and CCD lose their efficiency in UV range). However, the number of excited fluorescence transitions decreases with laser energy and red or even NIR excitations may seem more appropriate to prevent the Raman signal from being covered by the fluorescence one. The cost of the Raman set-up and the size of the optic path (i.e. of the size and weight of the spectrometer) are also important factors. Consequently green (532 nm) and red (785 nm) lasers often offer a good compromise. Note that for red (200-300 mW), a laser with higher power is usually required than for green (80-250 mW) laser excitation thanks to the associated decrease in Raman Effect and detector efficiency. Actually, a green laser can be preferred for inorganic materials: fluorescence in these compounds arises from Rare Earth traces (rather narrow peaks) or from pollution (biological surface film, especially for excavated samples). Ten to twenty mW at the sample is generally sufficient to clean the sample surface from biological films and its corresponding fluorescence. Obviously, the power of illumination should be adapted to the light absorption and heat transfer of the illuminated spot. Typically, a few μW can be sufficient to heat and modify black/heavy absorbent phases, but an optically clear colourless material can receive 1W without any heating!

Choice of the spectrometers

There is now a variety of "moving" instruments:

- i) The biggest and heaviest (>20Kg) are transportable and some-time require a screw to fix the co-secant bar (**Table 1**). Such instruments, like the Labram Infinity (Dilor, France) have been available since the 1990's.^{10,36} These instruments exhibit a high spectral resolution ($<2\text{ cm}^{-1}$), a flat background if gelatine Notch filters are used, can be equipped with horizontal or vertical microscopes, and can come with different exciting lasers incorporated. They are similar to many benchtop instruments (XY moving stage, large choice of objectives). An external power source is needed (often just an electric plug). And protection from ambient light (and eyes safety for the examiner) is achieved by closing the instrument doors.

- ii) The second class of mobile spectrometer connects independent parts (laser, spectrometer, remote head, XYZ stage) with the help of optic fibres, the spectrometer being the biggest and heaviest part ($\sim 10\text{ Kg}$ for 532 nm and $<5\text{ Kg}$ for 785 nm). The rejection of the Rayleigh scattering is obtained with Edge dielectric filters that give a complex background (first increasing regularly with wavenumber up to an inflexion point at $\sim 400\text{ cm}^{-1}$ and then a plateau). Spectral resolution is close to

3-4 cm⁻¹. Optics fibre length ranges from 3 to 30 m,^{32,36,43} and laser outputting power up to 300 mW are currently used. Typically, 1/10th of the out-put power reaches the sample. A variety of optics can be used. Electric plug connection or a mobile power supply unit are needed. A black textile is needed to suppress the ambient light and protect the examiner from the laser and scattered light (**Fig. 1**).

-ii) The last class of instruments are palm or handheld spectrometers. Some of them can be connected to a laptop for a better visualisation of the spectrum and its treatment.^{39,40,42} We won't consider here palm spectrometers for dedicated use (identification of liquid or solid chemicals and commodity) and giving direct identification of the analysed matter through specific software. The resolution of these instruments is limited (> 5 cm⁻¹) which render impossible the identification of the specific stretching modes of many sulphates, nitrates, carbonates, especially when they are mixed together in a corrosion layer. Furthermore, a baseline is automatically subtracted which makes the detection of broad components impossible. The lightness of these instruments (battery included) makes them very useful for field measurements (geology, building efflorescence, etc.). Generally, a (partially retractable) tube surrounds the optic and guaranties protection from ambient and laser/scattered light.

Choice of the optics

Although most know professional photographers choose their optics with caution, the selection of optics used in Raman set-up is often neglected by spectroscopists, which leads to the use of standard microscope objectives. Microscope objectives working in the visible range are optimised to give a better resolution in the xy plan than along the z axis: typically, the length along the z axis of the focused light's distribution (i.e. the spot volume) is 3 to 4 times larger than the spot diameter. Confocal diaphragm decreases this anisotropy but also very much the signal intensity. Furthermore, if optics fibres are used, the fibre core diameter determines the confocality.

Methods to measure the shape of the volume (in air) where the light is focused are well known.⁴⁵ Also note that the spectrometer may also contribute to the shape of the focused light spot. Furthermore, the volume size and shape are strongly enlarged in solids, and estimation/calculations are difficult since many parameters are not available.⁴⁶⁻⁴⁸ Thus, the choice of high quality and high magnification objectives is very beneficial as it widens the analysed volume in dielectric medium. The penetration depth depends on the absorption coefficient: for black and heavy coloured matter, the penetration depth can be less than a micron or even a few tenths of nm.⁴⁸

Another very important parameter is the working distance, i.e. the distance between the front lens and the focus point. Standard microscope objectives have short working distance in order to

maximise the angular volume of light collection (or in other words the numerical aperture). In that case, the sample-to-lens distance can be less than 1 mm for a x100 microscope objective. This is sufficient to analyse a polished sample but not to study an object with a complex shape such as one made of concave and convex regions separated by a cm or more. Objectives with long working distance are needed (**Fig. 2**). Increasing the working distance implies widening the lenses and hence drastically increasing the cost of the objective: typically the cost of a 20 mm LWD objective is 3 to 10 times that of a standard 3 mm x50 objective. When the Raman set-up cannot be protected from ambient light, the optical efficiency becomes very important, and a low numerical aperture an advantage! However the analysed surface should be exactly perpendicular to the optics axis to make the collection of the scattered light efficient.

The human eye's resolution being close to 2-10 μm , preparation of homogeneously coloured matter requires the use of smaller grains. If grains of different compositions are mixed together and if some grains generate fluorescence, it becomes necessary to study each grain individually, as to avoid a masking of the Raman signal by the fluorescence. Hence it was reported that using an x200 Mitutoyo objective (spot waist < 0.5 μm , i.e. close to the diffraction limit⁴⁸) renders possible the identification of a drawing's pigment regardless of the paper's huge fluorescence under green excitation.⁴⁹ Complex multicoloured décors for potteries are made by using a succession of thin glaze layers (the thickness being close to 10-20 μm , i.e. larger than the z-size of the focused spot obtained with x50 or even x100 microscope objective) and taking into account the broadening of the spot within the silicate glass. **Fig. 3** compares the Raman spectra (as recorded, not expanded) collected on the same enamelled *wucaí* porcelain with x50 (Nikon) and x200 (Mitutoyo) LWD objectives.^{50,51} The highest intensity of the Raman signature of both the crystalline (pigments) and amorphous (glaze matrix) phases recorded with a x200 objective is obvious.

As mentioned above, standard objectives have been designed for the visible range and special grade optimised for IR/NIR should be used outside of the visible range.¹³

Choice of the support - Stability

The high magnification optics required for Cultural Heritage studies implies a very good stability of the studied artefact and of the laser spot (i.e. of the optics). Heavy stage or support with micron-controlled displacements as illustrated in **Fig. 1** can be used. Examination can be made horizontally or vertically according to the shape and size of the studied artefact and the recommendation of the curator. Note the great efficiency of paper sheet rams in suppressing vibrations and adjusting the position very precisely. Heavy steel pieces are added to make the stage and the object support very

stable. It is important to also add pieces of foam to protect the artefact in the eventuality of falls (Fig. 1). Special supports are also required for some artefacts.^{52,53}

Intensity measurements and background subtraction

The variation of the Raman cross-section is very large because it depends on the bond polarizability that is a function of the covalence degree of the bond and of the number of electron involved.⁴⁷ The architecture of transportable/mobile instruments is based on the use of Notch or Edge filters. As mentioned above, the flat behaviour of the background generated by High Quality Notch filters facilitates subtractions/corrections. The two-segment shaped background of Edge dielectric filtering is sensitive to the colour of the analysed matter because of scattered light absorption. For example, the background almost disappears for blue glass analysed with green excitation [**Fig. 3**]. On the other hand stronger backgrounds are measured for red or colourless glass pieces.

The intensity of the spectrum is also an important parameter that can be used for the relative dating of glassy silicates. It has been pointed out that the degradation of the upper surface of glass pieces (microcracking, lixiviation, water/OH insertion ...) alters the optical quality of the surface and hence the laser penetration and scattered Raman signal (**Fig. 4 a & b**). The comparison of the band intensity makes possible the discrimination between glass produced during 20th, 19th, 18th etc.^{43,49} centuries. In the same way, the Raman signature of protonic species (water, OH⁻ groups, ...) collected in the 3000-3700 cm⁻¹ range (at the very surface of glass) (Fig. 4c), and the down-shift of the SiO₄ stretching peak, can be an indication of aged lixiviated glass/glaze^{54,55} as clearly demonstrated by Rutherford Backscattering Spectroscopy (RBS) for some objects made of quartz⁵⁶. Measurements on an ancient (excavated) porcelain from the surface to the bulk already shows broad and weak features with decreasing intensity from the surface to the glaze centre: these very weak bands can be assigned to water (3200 cm⁻¹) and hydroxyl groups (3700 cm⁻¹) that have diffused through the open porosity/cracks and/or in the glassy network. We can see that these bands are only detected in the glaze, not in the body. One can expect that both their intensity and gradient from the glaze surface to the bulk may help to discriminate between modern and old artefacts. These parameters will vary relative to the conservation condition and glaze composition, and further calibrations will be required.

Crystalline phase identification (Reference spectra & databases)

Reference works and databases such as those established for the Lunar Exploration Program,⁵⁷ and for gemmology,^{58,59} as well as by RUFF⁶⁰ or others⁶¹⁻⁶⁸ can be used to identify crystalline phases. Two

points should be considered: as colours matter, pigment Raman analysis is subject to Raman resonance that drastically modifies the band intensity (only modes related to the chromophore remain strong, see for example the evolution of the spectrum of Cr-doped sphené⁶⁹) and makes overtones and positive and negative combinations sufficiently strong to be visible.⁶⁹⁻⁷² Band position shift is generally small (a few cm^{-1}). In that case the efficiency of the database is poor. The use of high magnification microscope objectives allows for single grain analysis. In that case, the recorded spectrum is more or less strongly polarized and band intensity can be rather different from those of the database. A comprehensive study of artefacts rather similar to those studied on-site should be conducted at the laboratory with advanced instrument(s), and excited with different wavelengths before any on-site measurement campaigns. However, a visual identification by the examiner of the (poor) Raman signal collected on site during the focus adjustment is first required to choose if more spots should be tested or the signal recorded. Obviously, the adjustment of the focus with a high magnification microscope objective is more delicate and time consuming than with a standard objective. Thus, a choice should be made between the numbers of spectra collected (representativity) and their quality. In many cases, the best results are obtained by first adjusting the focus in the dark at a very low level of laser power (the spot should appear very sharp) and then increasing the laser's power up to the visualisation of the "good" Raman signature on the computer screen (Fig. 1).

Identification of amorphous silicates (glass and glaze). Broad band detection.

The identification of an amorphous silicate is of great interest in the study of enamelled and glass/pottery artefacts. Pigments and colouring ions are commonly dispersed in a glass to colour enamels. And some paintings' pigments are made of coloured glass grains. Although most pigments exhibit a Raman signature made of narrow peaks easily detectable even at low intensities, the spectrum of a glassy silicate consists in broad features: at around 1000 cm^{-1} for the SiO_4 symmetric stretching modes, at $\sim 550 \text{ cm}^{-1}$ for the bending ones and below 300 cm^{-1} for the so-called Boson peak (combination of very broad 'lattice' and librational modes⁷³⁻⁷⁶). In the past, the study of glassy silicates was restricted to very limited compositions only interesting geologists or physicists. As opposed to, because of the variety of substrates, the firing temperature, the thermal expansion, and the colour should be modified, and potters and glass makers may experiment with a huge variety of glassy compositions, from very depolymerised lead-rich glass melting below 600°C to very refractory, 3D-polymerised porcelain glaze melting above 1450°C . The study of the Raman signature of all the glassy silicates led to the introduction of a simple description of the stretching and bending of SiO_4 band intensity and components.⁷⁵ This modelling allows identifying the silicate composition and

melting temperature,⁷³ description valid for both crystalline and amorphous silicates.⁷⁶ Hence as sketched in **Fig. 5**, the ratio of the area of the SiO₄ bending modes divided by the area of the stretching modes depends on the polymerisation degree: continuous for glassy silicates and step by step for crystalline phases. Similar features are observed for phosphates and expected for other polymerized networks⁷⁷. Because the symmetric stretching mode of SiO₄ tetrahedrons is much stronger than the asymmetric one, the stretching band can be decomposed in 5 components, each of them assigned to isolated (Q₀) and connected tetrahedrons (by 1, 2, 3 or 4 oxygen atoms). The Raman signature of silicate is really the fingerprint of its polymerised network.

3. Study of refractory (inorganic) materials - Examples

We will discuss three examples: the identification of blue colouring agent(s), the opacification in white of enamelled glass and porcelains, and the study of corrosion layers. All examples point out that non-invasive Raman analysis provides very valuable data to document the ancient technologies of production and to follow the associated transfers of knowledge.

Blue glaze

For a long time, it has been postulated that only cobalt ions can colour blue silicates. In 1997 Clark & Laganara detected (at the laboratory) the very particular resonant Raman spectrum of S₂⁻ and S₃⁻ ions (the chromophores of lapis lazuli) in the glaze of rare enamelled faience shards excavated from Frederician-Normand famous sites (14th century, Castel del Monte, Lucera, Apulia, Italy).⁷⁸ In 1998 Anderson *et al.*⁷⁹ noted that they could not detect cobalt by SEM-EDS in some 13th-14th century blue Islamic enamel on glass. They did not pay attention to Raman publications. In 2003 Colomban⁷⁰ identifies the presence of both lapis lazuli grains (by Raman scattering) and cobalt (by SEM-EDS, 0.9% at) in a very common Lajvardina ewer (13th century, Iran): surprisingly both colouring agents were present in a very common production, although only one was sufficient to give the ultramarine hue and lapis lazuli was considered a rare compound. Lapis lazuli was then Raman detected in small fragments of a famous Roman "Lübsow" beaker (mostly destroyed in the bombing of the museum hosting it during the 2nd World War⁸⁰). In 2011, a Bari University group detected lapis lazuli in some shards of Ptolemaic faiences.⁸¹ This led us to conduct on-site measurement campaigns on the collections of Islamic enamelled glass at the Louvre and Art décoratifs museums in Paris, and on unique Ptolemaic Begram Hoard (Musée national des arts asiatiques –Guimet, Paris).^{52,53} The ongoing renovation of the Islam Department of the Louvre Museum made possible the access to one of the most outstanding collection of Mamluk mosque lamps and bottles. All blue enamels are coloured

with lapis lazuli as well as many green ones. Similar features were observed for pieces of glass excavated from Swabian-Normand sites^{82,83} demonstrating the very common use of lapis lazuli as a blue glass/glaze pigment. More amazingly, lapis lazuli was detected in the "white" glaze of the first hard-paste porcelain produced in Europe by J.F. Böttger in Saxony (Meissen, ~1720-1725).⁸⁴ However, the purity of the kaolin was not very good, and the achieved porcelain body was gray and not white. The glaze was only opacified with a dispersion of small bubbles. The dispersion of lapis lazuli grains in the glaze shifted the hue from gray to white, as the addition of blue dye in modern washing machine powder gives the illusion of a perfectly whitened textile. The same technique was used by linen Dutch merchants with the addition of small grains (cobalt blue coloured glass).

White opacification

There are many technical solutions to opacify a glaze. All of them use the dispersion of a phase with an optical index different from the matrix. The main opacifiers are tin oxide (cassiterite), calcium silicate (wollastonite), calcium phosphate and lead arsenate.⁷ Raman microspectrometry can very easily detect lead arsenate thanks to the high number of electron involved in the As-O bond. Lead arsenate is a very efficient opacifier of glass. It was first used by Venitian glassmakers to produce 'lattimo'^{85,86} and by Perrot to produce 'opaline' glass pieces at Orléans.⁸⁷⁻⁸⁹ But the high toxicity of arsenic has limited the development of the technology. Recent on-site studies of European soft-paste porcelains and faience^{90,91} and of Limoges enamels⁹² demonstrated that lead arsenate was present in blue enamels. This arises from the use of cobalt arsenide to colour the glass, cobalt arsenides being the common mineral ores of the Erzgebirge mines in Saxony.⁹³⁻⁹⁵ Arsenic from cobalt ore reacts with the lead-based glaze and lead-based arsenate precipitates and opacifies the glass. Small shifts in the As-O stretching band may indicate that a complex solid solution (K/Ca substitution) is formed. On the contrary, Asian cobalt ores have a very different geological origin (ancient sea nodules) and are manganese and iron rich and almost free of arsenic.⁹⁴ This offers a way to distinguish the use of cobalt ores. Both French and Chinese historical records report that enamelling know-how and French and Italian craftsmen expert in glass production and enamelling went to the Qing court under the guidance of Jesuits and contributed to the production of enamelled artefacts at the Beijing Palace.⁹⁶⁻⁹⁸ On-site analyses of very rare *huafalang* items – which, based on the style, seem to have been fired at the Imperial Court Workshop during the end of the Kangxi reign (~1715-1722) – identify lead arsenate in blue décor. The identification of lead arsenate in blue enamel only demonstrates the use of European cobalt ore, a proposal confirmed by elemental composition analysis of some *wucai* shards.⁹⁹⁻¹⁰¹ Rather similar bowls produced at the same workshop and period show different features, thus demonstrating a period of intense innovation. Lead can be partially

substituted by potassium or calcium giving complex solid solutions and some variety in the Raman signature.¹⁰²

The centre of gravity of bending and stretching SiO₄ bands can be used to identify the composition of the glassy silicate.⁷³⁻⁷⁶ Hence, considering the spectra of enamelled Yixing stoneware teapots (Fig. 3), the centre of gravity of dark blue and white enamel is at ~1020 cm⁻¹ and that of yellow glaze at ~980 cm⁻¹, according to a lower melting/firing temperature thanks to the larger lead content required to precipitate lead-based pyrochlore pigments. Other examples of how much information on glass and potteries production technology can be extracted from Raman spectra can be found considering ancient production¹⁰³⁻¹⁰⁵ but also Art Nouveau/Liberty and Modern ones.^{71,106,107}

Corrosion layers

On-site Raman analysis also is very efficient in identifying the inorganic phases of corrosion layers and patina on metal. Measurements performed on coupons at the laboratory have demonstrated their potential, in particular for the detection of amorphous or poor crystalline phases hardly detectable by x-ray diffraction and very detrimental to metal conservation.¹⁰⁸⁻¹¹² For instance, the corrosion layer of iron and steel is formed by different iron (oxy-hydroxides) that acts - or not - as a barrier and provides – or not – a protective ability. In order to check the conservation state through the protective capabilities, it is necessary to calculate the so-called protective ability index (PAI)^{113,114}. It mainly considers the ratio (α/γ) between the mass of goethite (α -FeOOH) and lepidocrocite (γ -FeOOH) present in the rust layer. The sensitivity of Raman spectroscopy for low crystallized phases and the microscopic resolution fulfils the requirements for PAI's calculations for complex and heterogeneous corroded layers. Madariaga's group demonstrated at the laboratory and with appropriate software¹¹⁵ that the portable spectrometer is very useful to select the most representative spots for sampling and comprehensive study.¹¹⁵⁻¹²³

Stone and plaster corrosion are also important questions where Raman studies can help understand mechanisms and solve problems. Using measurements being made at the laboratory on sampled fragments, Morillas *et al.*¹²¹⁻¹²³ showed that a combination of XRF and Raman on site measurements is sufficient to draw conclusions. A rather similar approach can be taken for bronze artefacts⁴⁴ and for glass⁵⁵ (but at smaller scale).

4. Paintings, drawings and mixed organic/inorganic materials - Examples

We will detail three examples of attempts to identify colouring agents and binders: in a wood panel painting (16th century),¹⁴ in a modern Italian paintings¹²⁴ and in Vietnamese and Japanese lacquerwares¹²⁵. In all three cases, 785 and 532 nm mobile set-ups, as well as a portable IR instrument, were used. The remote head associated to the 785 nm had a camera to visualise the illuminated spot and to choose the place of analysis (Fig. 6). Note that the thickness of the coloured layers (10 to 80 μm , typically) is similar regardless of material: glaze on glass or pottery and pictorial layer on canvas or wood (Fig. 7). This explains the interest in using high magnification microscope objectives. Attempts to measure directly the coloured layer only succeed for lacquerwares (identification of rutile, vermilion, cassiterite, chrome-orange and phthalocyanine)¹²⁴ with a 785nm excitation. The high quality of the lacquerware surface (very flat, high gloss) certainly helped the collection of in situ Raman scattered light. On-site measurements were only successfully performed on scales that fell down from the wood panel. The studied scales were put in grooves made on a metallic support in order to have the section ready for optical analysis: litharge, minium, and azurite were detected with a 532nm mobile Raman set-up. On the other hand, using a 785nm (transportable) instrument, 12 ingredients (white lead, calcite, vermilion, minium, azurite, indigo, lapis lazuli, calcite, gypsum) were identified in different hues, which compares favourably to the 10 and 8 compounds identified with 633 (transportable) and 1064 nm (fixed) ones respectively.¹⁴

In most cases, fluorescence prevented the procurement of a Raman spectrum through the varnished surface for the instrument with a 532nm laser source, while the 785 nm one equipped with a camera helping the selection of analysed spots succeeded in identifying only part of the pigments. As expected, Raman measurements on section, and especially those with 633 and 785 nm exciting laser lines, were effective to determine a high number of (organic or mineral) compounds employed for the artwork. Confocality of the instruments, and more important the use of high quality, high magnification, microscope objectives (x100 or x200) are very helpful (thanks to their very high lateral resolution) in limiting the fluorescence arising from the material surrounding the studied grain, and, allow for the complete characterization of the different layers of the pictorial stratigraphic sections. Use of optimised optics for the collected wavelength range is also important. Note that the majority of previous studies regarding paintings used one or two laser lines, which explains their very limited number and content, and that no attempts to use mobile set-ups was really made.

With the ATR-FTIR technique, the bands concerning the support (wood, textile) were easily detected and the media used for the painting were identified (lacquer, polymers) on very small samples^{14,125}. When sampling or collecting sub-millimetre fragments that fell down from the painting is possible, the efficiency of portable ATR-FTIR instrument is the same as that of laboratory instruments. Infrared analyses in a specular reflectance (Reflectance) mode using - or not - Kramers–Kronig Transformation

(KKT) to visualize the spectra gives good results for modern paintings. The large size of monocolour areas, the very small roughness and the high gloss of paintings are important advantages. The very characteristic bands of a poly(acrylates and methacrylates), vinylic and alkyd resins as well as polysaccharides and proteins are easily identified.¹²⁵

Other representatives examples are listed in Table 2.¹²⁶⁻¹⁴⁵

5. Conclusion

The great potential of mobile Raman equipment, very useful in many fields of conservation sciences, is limited when dealing with objects which don't have a surface exhibiting a 'good' optical quality (e.g. porous, very corrugated or microcracked surface) or are made of heterogeneous matter containing a large amount of fluorescent materials like glues and varnishes. However, Raman scattering is an optical investigation technique. The high efficiency of modern CCD tends to make us forget this important characteristic. Consequently, the difficulty to get 'good' spectra is minimal for crystals (gems) having nice facet and maximal for rough/porous stones. If a camera is not needed to observe the focus point of homogeneous enamels, spot-by-spot observation of paint mixture is necessary to select 'nice' fluorescence-free grains.

The use of a variety of exciting wavelengths is mandatory to identify the different colouring agents. Consequently, conclusions obtained from single laser line measurements are generally not representative. However, the mechanisms behind the interaction between lights and coloured matter are complex, and a deep understanding of the phenomena is required. Raman scattering is not a 'simple' analytical technique.

6. Acknowledgments

The author thanks all colleagues, students as well as curators and head of all the institutions offering access to the masterpieces studied.

7. References

1. Th. Rehren, E.B. Push, A. Herold Glass coloring works within a copper-centered industrial complex in Late Bronze age Egypt, in *The Prehistory & History of Glassmaking Technology* edited, by P. Mc Cray, *Ceramics and Civilization Series Vol. VIII*, Kingery W.D., Series Ed. The American Ceramic Society, **1998**, Westerville, p. 227-239.
2. G. Artioli, I. Angelini, A. Polla A., Crystals and phase transitions in protohistoric glasses, *Phase Transitions* **2008**; *81*: 233-252.
3. Ph. Beaujard, *Les mondes de l'océan Indien*. Vol. 1, *De la formation de l'Etat au premier système monde afro-eurasien*. Vol. 2, *L'océan Indien, au cœur des globalisations de l'Ancien Monde (7e-15e siècles)*. Armand Colin, **2012**, Paris.
4. R. Finlay, The Pilgrim Art: The Culture of Porcelain in World History, *J. World History*, **1998**; *9*[2]: 141-187.
5. Ph. Colomban, F. Treppoz, Identification and Differentiation of Ancient and Modern European Porcelains by Raman Macro- and Microspectroscopy, *J. Raman Spectrosc.* **2001**; *32*[2]: 93-102.
6. H. Davy, *Some experiments and observations on the colours used in painting by the ancients*. *Phil. Trans. Roy. Soc.*, **1815**; *105*: 97-124.
7. Ph. Colomban, *Arts* **2013**; *2*[3]: 111-123 (doi :10.3390/arts2030111).
8. H.G.M. Edwards, P. Vandenabeele, *Philos. Trans. R. Soc. A* **2016**; *374*[2082]: 20160052.
9. I.M. Bell, R.J.H. Clark, *Spectrochim. Acta, Part A* **1997**; *53*[12]: 2159-2179.
10. D.C. Smith, *Spectrochim. Acta. A-Mol. & Biomol. Spectrosc.* **2005**; *61*[10]: 2299-2314.
11. P. Vandenabeele, H.G.M. Edwards, L. Moens, *Chem. Rev.* **2007**; *107*[3]: 675-686.
12. J.M. Madariaga, *Anal. Methods* **2015**; *7*[12]: 4848, 10.1039/c5ay00072f.
13. E. Stanzani, D. Bersani, P. P. Lottici, Ph. Colomban, *Vib. Spectrosc.* **2016**; *85*: 62-70.
14. P. Dhamelincourt, F. Wallart, M. Leclercq, A.T. Nguyen, D.O. Landon, *Anal. Chem.* **1979**; *51*[3]: 414A-420A.
15. Ph. Colomban, *L'Industrie Céramique* **1979**; *734*: 815-820.
16. M. Delhay, B. Guineau, J. Vezin, *Le Courrier du C.N.R.S.*, **1984**; *58*: 20-31.
17. B. Guineau, C. Coupry, M.-T. Gousset, J.-P. Forgerit, J. Vezin, *Scriptorium* **1986**; *XL*[2]: 157-171.
18. R.J.H. Clark, *Chem. Soc. Rev.* **1995**; *24*[3]: 187-196.
19. S. Panayotova, D. Jackson, P. Ricciardi, *Colour, the art & science of illuminated manuscripts*, Harvey Miller Publishers, London, **2016**.
20. A. Barbet, C. Coupry, A. Lautie, Apport de la spectrométrie Raman à la caractérisation de peintures murales, in *Roman Wall Painting Materials, Techniques Analysis and Conservation*, Proceedings of the International Workshop, Fribourg, 7-9 March 1996, Fribourg, **1997**, p. 257-268.
21. H.G.M. Edwards, E.M. Gwyer, J.K.F Teit, *J. Raman Spectrosc.* **1997**; *28*[9]: 677-684.
22. A. Rosalie-David, H.G.M. Edwards, D.W. Farrell, D.L.A. de Faria, *Archaeometry* **2001**; *43*[4]: 461-473.
23. P. Baraldi, A. Bonazzi, N. Giordani, F. Paccagnella, P. Zannini, *Archaeometry* **2006**; *48*[3]: 481-499.
24. A. Brysbaert, P. Vandenabeele, *J. Raman Spectrosc.* **2004**; *35*[8-9]: 686-693.
25. X. Wang, C. Wang, J. Yang, L. Chen, J. Feng, M. Shi, *J. Raman Spectrosc.* **2004**; *35*[8-9]: 274-278.
26. D. Bersani, P. P. Lottici, G. Antonioli, E. Campani, A. Casoli, C. Violante, *J. Raman Spectrosc.* **2004**; *35*[8-9]: 694-703.
27. M. Sánchez del Río, M. Picquart, E. Haro-Poniatowski, E. van Elslande, V. Hugo Uc, *J. Raman Spectrosc.* **2006**; *37*[10]: 1046-1053.

28. Cl. Coupry, B. Palazzo-Bertholon, « Les pigments verts, rouges et bleus dans les décors peints de la fin de l'Antiquité et du haut Moyen Âge ». Actes du colloque, Décor et architecture en Gaule entre l'Antiquité et le haut Moyen Age : mosaïque, peinture, stuc, Aquitania, Suppl. 20, Bordeaux, **2011**, p. 689-698
29. L. Burgio, R.J.H. Clark, *Spectrochim. Acta, Part A*. **2001**; 57[7]: 1491–1521.
30. D.C. Smith, *Spectrochim. Acta. A-Mol. & Biomol. Spectrosc.* **2003**; 59[10]: 2353-2359.
31. Ph. Colomban, V. Milande, L. Le Bihan, *J. Raman Spectrosc.* **2004**; 35[7]: 527-535.
32. Ph. Colomban, V. Milande, H. Lucas, *J. Raman Spectrosc.* **2004**; 35[1]: 68-72.
33. M.A. Ziemann, *J. Raman Spectrosc.* **2006**; 37[10]: 1019-1025.
34. F. Immler, O. Schrems, *Geophys. Res. Lett.* **2002**; 29[16]: 1809-1811.
35. M. N. Abedin, A.T. Bradley, Arthur T.; S. Ismail, *Appl. Optics* **2013**; 52[14]: 3116-3126.
36. Ph. Colomban, *J. Raman Spectrosc.* **2012**; 43[11]: 1529-1535.
37. D. Lauwers, A.G. Hutado, V. Tanevska, L. Moens, D. Bersani, P. Vandenabeele, *Spectrochim. Acta, Part A* **2014**; 118: 294–301.
38. P. Vandenabeele, M.K. Donais, *Appl. Spectrosc.* **2016**; 70[1]: 27-41.
39. P. Vandenabeele, H.G.M. Edwards, J. Jehlička, *Chem. Soc. Rev.* **2014**; 43[8]: 2628-2649.
40. J. Jehlička, P. Vitek, H. G. M. Edwards, M. Hargreaves, T. Čapoun, *J. Raman Spectrosc.* **2009**; 40[11]: 1645–1651
41. L.V. Harris, I.B. Hutchinson, R. Ingle, C.P. Marshall, A.O. Marshall, H.G. M. Edwards, *Astrobiology* **2015**; 15[6]: 420-429
42. J. Jehlička, A. Culka, D. Bersani, P. Vandenabeele, Comparison of seven portable Raman spectrometers: beryl as a case study, *J. Raman Spectrosc.* DOI: 10.1002/jrs.5214.
43. Ph. Colomban, A. Tournié, *J. Cult. Herit.* **2007**; 8[3]: 242-256.
44. Ph. Colomban, A. Tournié, Ph. Meynard, M. Maucuer, *J. Raman Spectrosc.* **2012**; 43[6]: 799-808.
45. Ph. Colomban, *Spectroscopy Europe* **2003**; 15[6]: 8-15.
46. C. Sourisseau, *Chem. Rev.*, **2004**; 104[9]: 3851–3892
47. G. Gouadec, Ph. Colomban, *Prog. Cryst. Growth Charact. Mater.* **2007**; 53[1]: 1–56.
48. G. Gouadec, L. Bello-Gurlet, D. Baron, Ph. Colomban, Raman mapping for the investigation of nanophased materials, ch. 4, , *in* RAMAN IMAGING, TECHNIQUES & APPLICATIONS, A. Zoubir Ed., Springer Series in Optical Sciences, **2012**, Vol. 168, p 85-118.
49. D. Mancini, A. Tournié, M.-C. Caggiani, Ph. Colomban, *J. Raman Spectrosc.* **2012**; 43[2]: 294-302.
50. Ph. Colomban, Y. Zhang, B. Zhao, *Ceram. Int.* **2017**; 43[15]: 12079-12088.
51. Ph. Colomban, T.-A. Lu, V. Milande, *Ceram. Int.* submitted
52. Ph. Colomban, A. Tournié, M.-C. Caggiani, C. Paris, *J. Raman Spectrosc.* **2012**; 43[12]: 1975-1984.
53. M.C. Caggiani, Ph. Colomban, A. Mangone, C. Valloteau, P. Cambon, *Anal. Methods*, **2013**; 5[17]: 4345-4354.
54. Ph. Colomban, M.-P. Etcheverry, M. Asquier, M. Bounichou, A. Tournié, *J. Raman Spectrosc.* **2006**; 37[5]: 614–626.
55. A. Tournié, P. Ricciardi, Ph. Colomban, *Solid State Ionics* **2008**; 179[38]: 2142-2154.
56. Th. Calligaro, Y. Coquinot, I. Reiche, J. Castaing, J. Salomon, G. Ferrand, Y. Le Fur, *Appl. Phys. A* **2009**; 94[4]: 871–878.
57. W.P. Griffith, Raman Spectroscopy of Terrestrial Minerals, in *Infrared and Raman Spectroscopy of Lunar and Terrestrial Minerals*, C. Karr Jr Ed., **1975**, New York, Academic Press.

58. Maestrati R., 1989, *Contribution à l'édification du catalogue Raman des gemmes*, Diplôme d'Université de gemmologie, Université de Nantes.
59. Pinet M., Smith D.C., Lasnier B., Utilité de la microsonde Raman pour l'identification non-destructive des gemmes, in *La Microsonde Raman en géologie*, *Revue de gemmologie* **1992**; juin, numéro hors-série.
60. <http://rruff.geo.arizona.edu/rruff/> (accessed 12th August 2017)
61. <http://minerals.gps.caltech.edu/files/raman> (accessed 12th August 2017)
62. <http://www.ens-lyon.fr/LST/Raman/index.php> (accessed 12th August 2017)
63. http://sdfs.db.aist.go.jp/sdfs/cgi-bin/cre_index.cgi (accessed 12th August 2017)
64. <http://www.irug.org/search-spectral-database> (accessed 12th August 2017)
65. <http://www.fis.unipr.it/pheviz/ramandb.html> (accessed 12th August 2017)
66. <http://www.geologie-lyon.fr/Raman/> (accessed 12th August 2017)
67. <http://www.chem.ucl.ac.uk/resources/raman/index.html> (accessed 12th August 2017)
68. <http://chsopensource.org/2016/06/27/free-raman-database-of-pigments-checker/> (accessed 12th August 2017)
69. X. Faurel, A. Vanderperre, Ph. Colomban, *J. Raman Spectrosc.* **2003**; 34[4]: 290-294.
70. Ph. Colomban, *J. Raman Spectrosc.* **2003**; 34[6]: 420-423.
71. C. Fornacelli, Ph. Colomban, I. Turbanti Memmi, *J. Raman Spectrosc.* **2015**; 46[11]: 1129-1139.
72. F. Rosi, C. Grazia, F. Gabrieli, A. Romani, M. Paolantoni, R. Vivani, B. G. Brunetti, Ph. Colomban, C. Miliani, *Microchemical J.* **2016**; 124[1]: 856-867.
73. Ph. Colomban, *J. Non-Crystalline Solids* **2003**; 323[1-3]: 180-187.
74. Ph. Colomban, A. Tournié, L. Bellot-Gurlet, *J. Raman Spectrosc.* **2006**; 37[8]: 841-852.
75. Ph. Colomban, L.C. Prinsloo, Optical Spectroscopy of Silicates and Glasses, in *Spectroscopic Properties of Inorganic and Organometallic Compounds*, J. Yarwood, R. Douthwaite, S. B. Duckett Eds, RSC Publishing, The Royal Society of Chemistry, **2009**, Cambridge, pp 128-149.
76. Ph. Colomban, A. Slodczyk, *Optical Materials* **2009**; 31[12]: 1759-1763.
77. A. Tournié, UPMC PhD Dissertation, www.glv-t-cnrs.fr/ladir/pages/theses/These_Aurelie_Tournie.pdf.
78. R.J.H. Clark, M.L. Curri, C. Laganara, *Spectrochimica Acta Part A* **1997**; 53[4]: 597-603.
79. Anderson, Freestone & Stapelton in R. Ward, *Gilded and Enamelled Glass from the Middle East*, British Museum Press: London, **1998**.
80. S. Greiff, J. Schuster, *J. Cult. Herit.* **2008**; 9 Suppl.: e27-e32.
81. A. Mangone, G. E. De Benedetto, D. Fico, L. C. Giannossa, R. Laviano, L. Sabbatini, I. D. van der Werf, A. Traini, *New J. Chem.*, **2011**; 35[12]: 2860-2868.
82. M.C. Caggiani, P. Aquafredda, Ph. Colomban, A. Mangone, *J. Raman Spectrosc.* **2014**; 45[11-12]: 1251-1259.
83. M.C. Caggiani, N. Ditaranto, M.R. Gaschito, P. Acquafredda, R. Laviano, L.C. Gianossa, S. Mutino, A? Mangone, *X-Ray Spectrom.* **2015**; 44[4]: 191-200.
84. Ph. Colomban, V. Milande, *J. Raman Spectrosc.* **2006**; 37[5]: 606-613.
85. M. Verita S. Zecchin, Raw materials and glass making technology in nine Murano glasswork, teenth century, www.istitutoveneto.org/pdf/testi/vetro/.../02_verita_zecchin.pdf (accessed 12th August 2017)
86. P. Ricciardi, Ph. Colomban, A. Tournié, V. Milande, *J. Raman Spectrosc.* **2009**; 40[6]: 604-617.
87. J. Barrelet, *Cahiers de la céramique du verre et des arts du feu: Sèvres*, **1964**; 36: 254-26.
88. A. Bouthier, Bernard Perrot entre secret et innovations, Les Innovations Verrières et leur Devenir, Actes du 2è Colloque Verre et Histoire, Nancy, 26-28 March 2009 (http://www.verre-histoire.org/colloques/innovations/pages/p205_01_bouthier.html, Accessed 18th May 2017).

89. J. Geysant, *Secret du verre rouge transparent de Bernard Perrot et comparaison avec celui de Johann Kunckel*, Somogy-Editions d'Art, Paris, **2010**, pp. 51–54.
90. D. Mancini, C. Dupont-Logié, Ph. Colomban, *Ceram. Int.* **2016**; *42*[13]: 14918-14927.
91. Ph. Colomban, T.-A. Lu, V. Milande, to be published
92. Ph. Colomban, L. Arberet, B. Kirmizi, *Ceram. Int.* **2017**; *43*[13]: 10158-10165.
93. B. Gratuze, I. Soulier, M. Blet, L. Vallauri, *Rev. d'Archéométrie* **1996**; *20*: 77-94.
94. Ph. Colomban, *Eur. Mineralogy J.* **2013**; *25*[5]: 863-879.
95. R.G.V. Hancock, J. McKechnie, S. Aufreiter, K. Karklins, M. Kapches, M. Sempowski, J.F. Moreau, I. Kenyon, *J. Radioanal. Nucl. Chem.* **2000**; *244*[3]: 567–573.
96. F. Lili, *La céramique chinoise*, China Intercontinental Press, Beijing, **2011**.
97. B. Zhao, G. Wang, I. Biron, Ph. Colomban, L. Hilaire-Pérez, *Le Cnrs en Chine Bulletin*, **2016**; *21*: 21–25.
http://www.cnrs.fr/derci/IMG/pdf/cnrsenchine_21_fr_final_pour_le_site_cnrs.pdf (access 29th September 2017).
98. X.D. Xu, *Europe-China-Europe: the transmission of the craft of painted enamel in the seventeenth and eighteenth centuries*, in: Maxine Berg (Ed.), *Goods from the East, 1600–1800 Trading Eurasia*, Palgrave Macmillan, Houndmills, Basingstoke, Hampshire, **2015**, pp. 92–106.
99. R. Giannini, I.C. Freestone, A.J. Shortland, *European cobalt sources identification in the production of Chinese famille rose porcelain*, *J. Archaeol. Sci.* **2016**; *80*: 27–36.
100. J. Van Pevenage, D. Lauwers, D. Herremans, E. Verhaeven, B. Vekemans, W. De Clercq, L. Vincze, L. Moens, P. Vandenabeele, *Anal. Methods* **2014**; *6*: 387–394.
101. Ph. Colomban, F. Ambrosi, Anh-Tu Ngo, Ting-An Lu, Xiong-Lin Feng, Stephen Chen, Chung-Lit Choi, *Ceram. Int.* **2017**; *43*: <http://dx.doi.org/10.1016/j.ceramint.2017.07.172>
102. B. Manoun, M. Azdouz, M. Azrour, R. Essehli, S. Benmokhtar, L. El Ammari, A. Ezzahi, A. Ider, P. Lazor, *J. Mol. Struct.* **2011**; *986*: 1–9.
103. B. Kirmizi, Ph. Colomban, B. Quette, *J. Raman Spectrosc.* **2010**; *41*[7]: 780-790.
104. B. Kirmizi, Ph. Colomban, M. Blanc, *J. Raman Spectrosc.* **2010**; *41*[10]: 1240-1247.
105. G. Simsek, Ph. Colomban, F. Casadio, L. Bellot-Gurlet, K. Faber, G. Zelleke, V. Milande, L. Tilliard, *J. Am. Ceram. Soc.* **2015**; *98*[10]: 3006-3013.
106. M.C. Caggiani, C. Valloteau, Ph. Colomban, *Inside the glassmaker technology: Search of Raman criteria to discriminate between Emile Gallé and Philippe-Joseph Brocard Enamels and Pigment Signatures*, *J. Raman Spectrosc.* **2014**; *45*[6]: 456-464.
107. C. Fornacelli, Ph. Sciau, Ph. Colomban, *Phil. Trans. R. Soc. A* **2016**; *374*: 20160045
(<http://dx.doi.org/10.1098/rsta.2016.0045>).
108. D. Neff, S. Reguer, L. Bellot-Gurlet, P. Dillmann, R. Bertholon, *J. Raman Spectrosc.* **2004**; *35*[8-9]: 739-745.
109. L. Bellot-Gurlet, D. Neff, S. Réguer, J. Monnier, M. Saheb, P. Dillmann, *J. Nano. Res.* **2009**; *8*: 147-156.
110. S. Réguer, P. Dillmann, F. Mirambet, L. Bellot-Gurlet, *Nucl. Instr. Meth. Phys. Res. B.* **2005**; *240*[1-2]: 500-504.
111. Ph. Colomban, S. Cherifi, G. Despert, *J. Raman Spectrosc.* **2008**; *39*[7]: 881–886.
112. Ph. Colomban, *Potential and drawbacks of Raman (micro)spectrometry for the understanding of iron and steel corrosion*, Ch. 28 in *New Trends and Developments, in Automotive System Engineering*, M. Chiaberge Ed., INTECH, **2010**, pp. 567-564.
113. T. Kamimura, S. Hara, H. Miyuki, M. Yamashita, H. Uchida, *Corrosion Sci.* **2006**; *48*[9]: 2799-2812.
114. P. Dillmann, F. Mazaudier, S. Hoerlé, *Corros. Sci.* **2004**; *46*[6]: 1401-1429.

115. J. Aramendia, L. Gomez-Nubla, K. Castro, I. Martinez-Arkarazo, D. Vega, A. Sanz López de Heredia, A. García Ibáñez de Opakua, J.M. Madariaga, *J. Raman Spectrosc.* **2012**; *43*[8]: 1111-1117.
116. J. Aramendia, L. Gomez-Nubla, I. Arrizabalaga, N. Prieto-Taboada, K. Castro, J. M. Madariaga, *Corros. Sci.* **2013**; *76*: 154-162.
117. J. Aramendia, L. Gomez-Nubla, L. Bellot-Gurlet, K. Castro, C. Paris, Ph. Colomban, J. M. Madariaga, *J. Raman Spectrosc.* **2014**; *45*[11-12]: 1076-1084.
118. V. Matović, S. Eric, A. Kremenović, Ph. Colomban, D. Srecković-BatoVanin, N. Matović, *J. Cult. Herit.* **2012**; *13*[2]: 175-186.
119. V. Matović, S. Erić, A. Kremenović, Ph. Colomban, *Environmental Earth Sciences* **2014**; *72*[6]: 1939-1951.
120. V. Matović, A. Kremenović, Ph Colomban, D. Srećković Batoćanin, M. Nešković, A. Jelikić, *Construction & Building Materials* **2015**; *98*: 25-34.
121. H. Morillas, M. Maguregui, C. Paris, L. Bellot-Gurlet, Ph. Colomban, J. M. Madariaga, *Microchemical J.* **2015**; *123*: 148-157.
122. C. Garcia-Florentino, M. Maguregui, H. Morillas, U. Balziskueta, A. Azcarate, G. Arana, J.M. Madariaga, *J. Raman Spectrosc.* **2016**; *47*[12]: 1458-1466.
123. H. Morillas, J. Garcia-Galan, M. Maguregui, C. Garcia-Florentino, I. Marcaida, J.A. Carrero, J.M. Madariaga, *Microchemical J.* **2016**; *128*: 288-296.
124. Ph. Colomban, D. Mancini, *Arts* **2013**; *2*[3]: 111-123 doi:10.3390/arts2030111
125. D. Mancini, A. Percot, L. Bellot-Gurlet, Ph. Colomban, unpublished.
126. I. Reiche, S. Pages-Camagna, L. Lambacher, *J. Raman Spectrosc.* **2004**; *35*[8-9]: 719–725.Z.
127. Petrova', J. Jehlic'ka, T. Č'apoun, R. Hanus, T. Trojek, V. Golias, *J. Raman Spectrosc.* **2012**; *43*[9]: 1275–1280.
128. D. Lauwers, V. Cattersel, L. Vandamme, A. Van Eester, K. De Langhe, L. Moens, P. Vandenabeele, *J. Raman Spectrosc.* **2014**; *45*[11-12]: 1266–1271.
129. A. Deneckere, M. Leeftang, M. Bloem, C.A. Chavannes-Mazel, B. Vekemans, L. Vincze, P. Vandenabeele, L. Moens, *Spectrochim. Acta A.* **2011**; *83*[1]: 194–199.
130. P. Vandenabeele, J. Tate, L. Moens, *Anal. Bioanal. Chem.* **2007**; *387*: 813–819.
131. L. Van de Voorde, J. Van Pevenage, K. De Langhe, R. De Wolf, B. Vekemans, L. Vincze, P. Vandenabeele, M.P.J. Martens, *Spectrochim. Acta, Part B.* **2014**; *97*: 1–6.
132. D.C. Smith, A. Barbet, *J. Raman Spectrosc.* **1999**; *30*[4]: 319–324.
133. A. Deneckere, W. Schudel, M. Van Bos, H. Wouters, A. Bergmans, P. Vandenabeele, L. Moens, *Spectrochim. Acta, Part A.* **2010**; *75*: 511–519.
134. P. Vandenabeele, K. Lambert, S. Mattys, W. Schudel, A. Bergmans, L. Moens, *Anal. Bioanal. Chem.* **2005**; *383*[4]: 707–712.
135. P. Vandenabeele, L. Moens. "Raman Spectroscopy: New Light on Ancient Artefacts". In: J. Nimmrichter, W. Kautek, M. Schreiner (Eds), *Lasers in the Conservation of Artworks*. Berlin, Germany: Springer, **2007**, pp. 341–347.
136. P. Vandenabeele, R. Garcia-Moreno, F. Mathis, K. Leterme, E. Van Elslande, F.-P. Hocquet, S. Rakkaa, D. Laboury, L. Moens, D. Strivay, M. Hartwig, *Spectrochim. Acta A.* **2009**; *73*: 546–552.
137. A. Bonneau, D.G. Pearce, A.M. Pollard, *J. Arch. Sci.* **2012**; *39*[2]: 287–294.
138. A. Tournié, L.C. Prinsloo, C. Paris, P. Colomban, B. Smith, *J. Raman Spectrosc.* **2011**; *42*[3]: 399–406.
139. L.C. Prinsloo, A. Tournié, P. Colomban, C. Paris, S.T. Bassett, *J. Arch. Sci.* **2013**; *40*[7]: 2981–2990.
140. M. Olivares, K. Castro, M.S. Corcho' n, D. Ga'rate, X. Murelaga, A. Sarmiento, N. Etxebarria, *J. Arch. Sci.* **2013**; *40*[2]: 1354–1360.
141. S. Lahlil, M. Lebon, L. Beck, H. Rousselière, C. Vignaud, I. Reiche, M. Menu, P. Paillet, F. Plassard, *J. Raman Spectrosc.* **2012**; *43*[11]:1637–1643.
142. H. Morillas, M. Maguregui, O. Go'mez-Laserna, J. Trebolazabala, J.M. Madariaga, *J. Raman Spectrosc.* **2012**; *43*[11]: 1630–1636.
143. I. Martínez-Arkarazo, A. Sarmiento, M. Maguregui, K. Castro, J.M. Madariaga, *Anal. Bioanal. Chem.* **2010**; *397*[7]: 2717–2725.

144. J. Aramendia, L. Gomez-Nubla, K. Castro, I. Martinez- Arkarazo, D. Vega, A. Sanz Lo´pez de Heredia, A. Garcia Iba´n˜ez de Opakua, J.M. Madariaga, *J. Raman Spectrosc.* **2012**; *43*[8]: 1111–1117.
145. M. Maguregui, U. Knuutinen, I. Mart´ınez-Arkarazo, A. Giakoumaki, K. Castro, J.M. Madariaga, *J. Raman Spectrosc.* **2012**; *43*[11]: 1747–1753.

FIGURE CAPTIONS

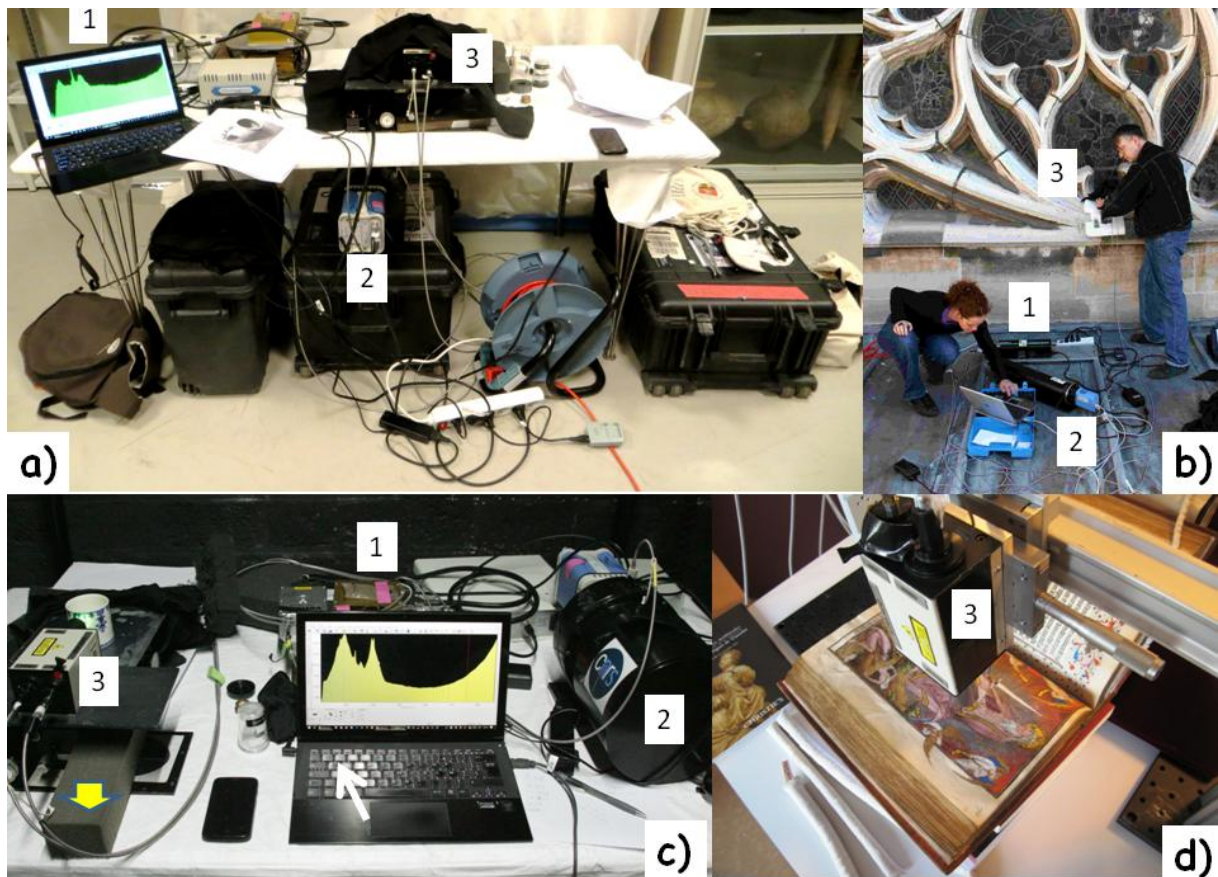


Fig. 1: Advanced mobile Raman set-up used in Museum (a,c) and Library (c) storage rooms and on the roof of Sainte-Chapelle, Palatine Church, Paris (b). Laser (1), spectrometer (2) and fibre optics connected remote head are labelled (3). See refs ⁴³ and ⁷⁷ for details. Note the heavy piece of steel to stabilise the xyz stage (c) (yellow arrow).

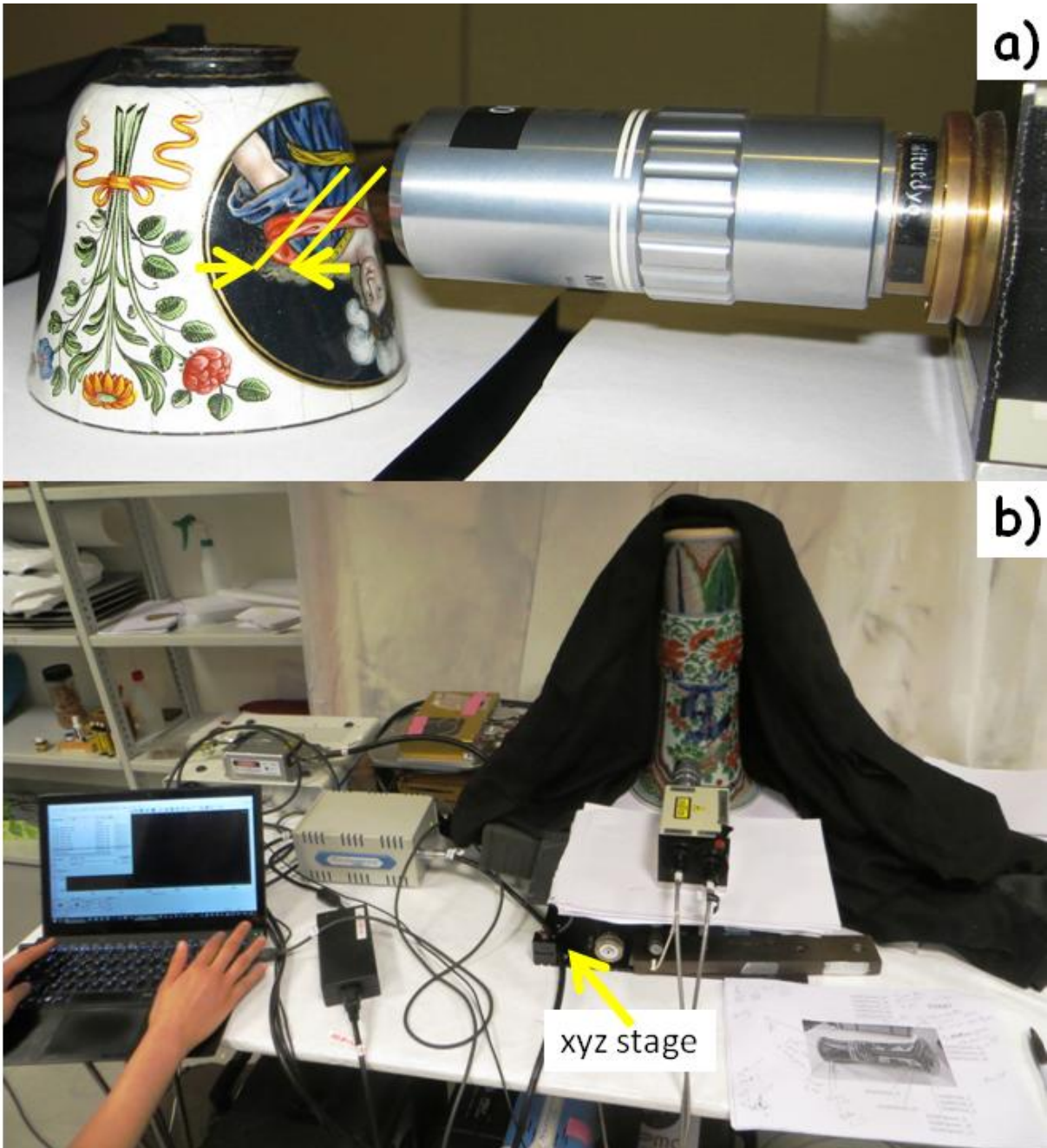


Fig. 2: Analysis of a) an enamelled goblet (18th century Limoges Laudin family workshop) and b) of a *wucui* Chinese porcelain vase using a high magnification (x200) long working distance (13 mm) microscope objective (see refs ⁹² and ¹⁰⁴ for details); note the paper sheets used to protect from vibrations and to adjust the position of the spot in complement with the xyz stage; b) the black textile covers the remote head and the artefact during the measurement.

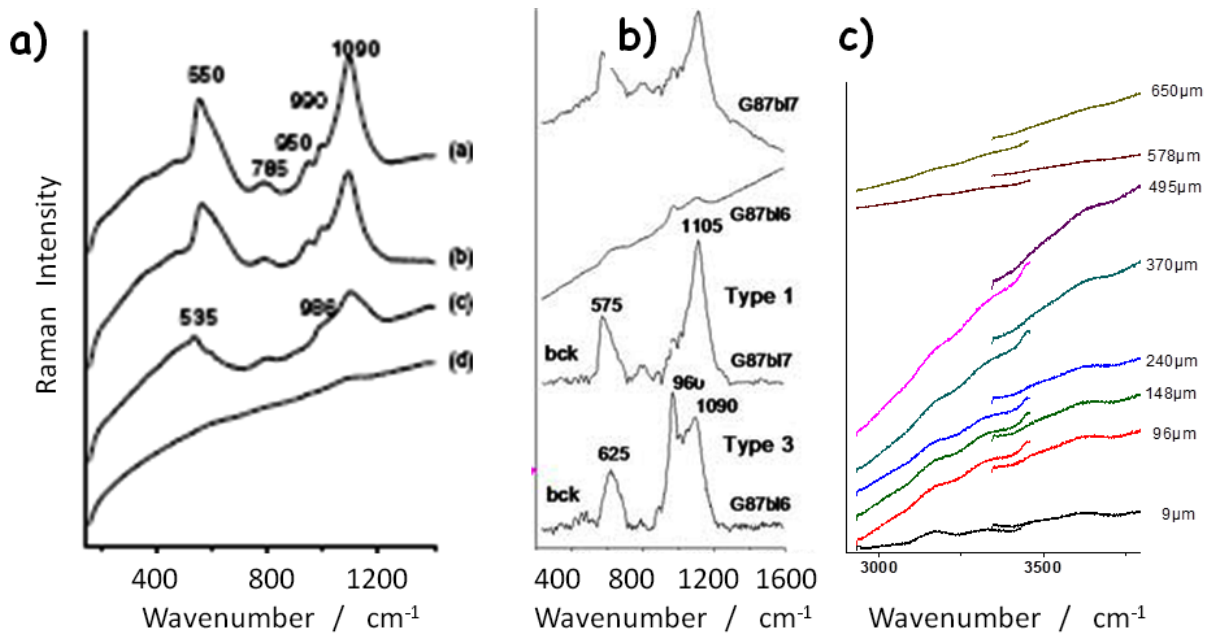


Fig. 4: Comparison of spectra recorded with the same conditions, the absolute intensity decreasing with the age of the artefacts: a) modern (1,2), 19th (3) and 18th century (4) glass of ancient miniatures (after ref. ⁴⁹) and b) medieval potash (Type 3) and 19th century restored soda-lime (Type 1) stained glass (as recorded and after baseline subtraction and normalisation (bck), after ref. ⁴³); c) see the ca. 3200 (adsorbed water) and 3600 cm⁻¹ (OH groups) signatures of protonic species trapped in the glaze layer can be also used to compare the age of different objects (conserved in similar conditions); here the spectra have been regarded at different places on fracture, from the very surface to the glaze/body interface (~500 μm).

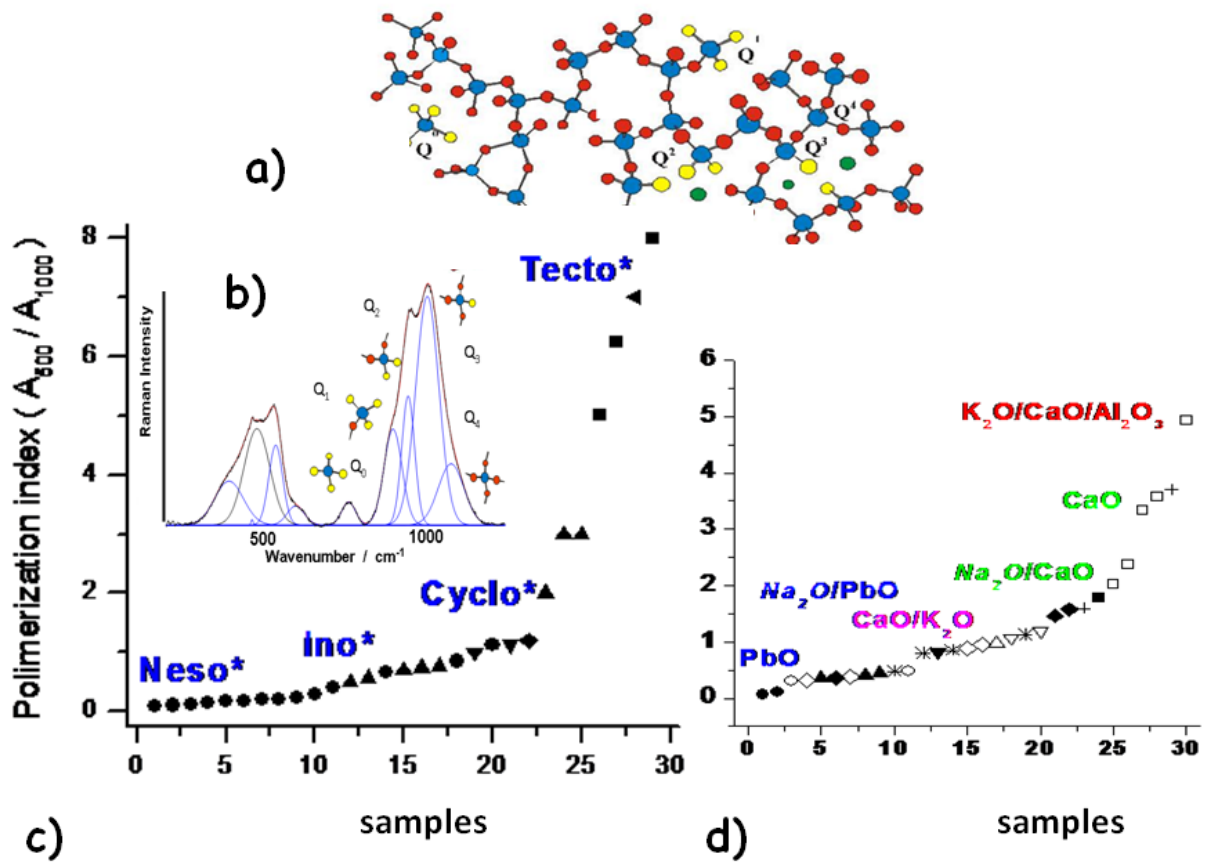


Fig. 5: a) Schematic of the glass polymeric network made of more or less connected SiO_4 tetrahedron with fluxing ions in between; b) Typical Raman spectrum showing the stretching and bending components relative of the different types of tetrahedron (Q_0 , isolated to Q_4 full connected), the Boson contribution has been subtracted (see in refs ⁷³⁻⁷⁵ for details). Plot of the polymerization index (ratio of the bending vs. stretching band area) for crystalline (c) and amorphous (d) silicates; the main flux and other oxides are indicated, after ref. ⁷⁶.

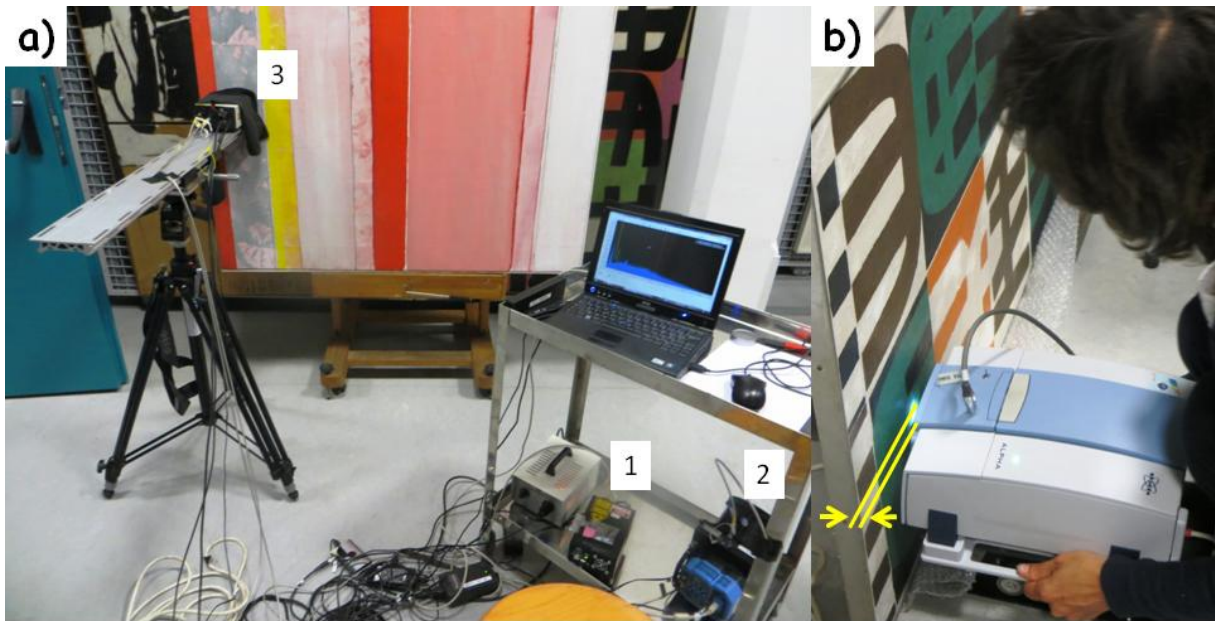


Fig. 6: On-site measurement of modern paintings using HE785 Raman (a) and FT-IR spectrometer (b).

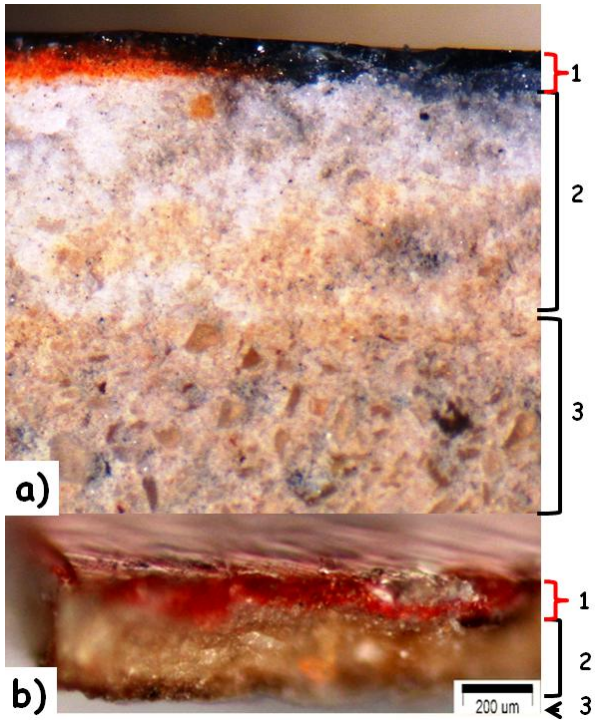


Fig. 7: Comparison of sections (fracture) of a pottery (Iznik fritware) and of a pictorial layer (wood panel) showing the rather similar thickness of the coloured layers (1), here deposited on a quartz grain-rich slip (2, a) or a calcite/gypsum preparation layer (2,b), (3) fritware and wood substrate)

Table 1: Representative characteristics of spectrometers used for Cultural Heritage studies

Characteristics	Transportable	Mobile	Mobile	Handheld
Spectral range (cm ⁻¹)	60-4000	80-3300	100-3200	200---2500 (or less)
Laser line	532,633	532	785	785
Optics	up to x100	up to x200	up to x100	<x20
Baseline	linear	complex	complex	Automatically 'corrected'
Weight (Kg)	>50	>15	<10	<2

Table 2: Examples of on-site studies with (trans)portable Raman set-ups.

Materials	References
Gemstones	30,33,37,40,41,126,127
Pigments of illuminated manuscripts	48,128,129
Wall paintings & frescoes	130,132-136,145
Rock art	137-141
Buildings & stones	121-123,142,143
G lass, glaze & pottery	31,32,43,49,50,52,53,90,92,101,103-106
Bronze corrosion & patina	44
Iron/steel corrosion layer & patina	116,117,144
Paintings pigments	13,124,131
Lacquerware pigments medium	125